Dalton Transactions

Cite this: *Dalton Trans.*, 2011, **40**, 9413

www.rsc.org/dalton

PAPER

Nickel(II) complexes of tripodal 4N ligands as catalysts for alkane oxidation using *m*-CPBA as oxidant: ligand stereoelectronic effects on catalysis†

Mani Balamurugan,[a] Ramasamy Mayilmurugan,[a] Eringathodi Suresh[b] and Mallayan Palaniandavar*[a]

Received 12th May 2011, Accepted 11th July 2011
DOI: 10.1039/c1dt10902b

Several mononuclear Ni(II) complexes of the type $[Ni(L)(CH_3CN)_2](BPh_4)_2$ **1–7**, where L is a tetradentate tripodal 4N ligand such as *N*,*N*-dimethyl-*N*′,*N*′-bis(pyrid-2-ylmethyl)ethane-1,2-diamine (**L1**), *N*,*N*-diethyl-*N*′,*N*′-bis(pyrid-2-ylmethyl)ethane-1,2-diamine (**L2**), *N*,*N*-dimethyl-*N*′-(1-methyl-*1H*-imidazol-2-ylmethyl)-*N*′-(pyrid-2-ylmethyl)ethane-1,2-diamine (**L3**), *N*,*N*-dimethyl-*N*′,*N*′-bis(1-methyl-*1H*-imidazol-2-ylmethyl)ethane-1,2-diamine (**L4**), *N*,*N*-dimethyl-*N*′,*N*′-bis(quinolin-2-ylmethyl)ethane-1,2-diamine (**L5**), tris(benzimidazol-2-ylmethyl)amine (**L6**) and tris(pyrid-2-ylmethyl)amine (**L7**), have been isolated and characterized using CHN analysis, UV-Visible spectroscopy and mass spectrometry. The single-crystal X-ray structures of the complexes $[Ni(L1)(CH_3CN)(H_2O)](ClO_4)_2$ **1a**, $[Ni(L2)(CH_3CN)_2](BPh_4)_2$ **2**, $[Ni(L3)(CH_3CN)_2](BPh_4)_2$ **3** and $[Ni(L4)(CH_3CN)_2](BPh_4)_2$ **4** have been determined. All these complexes possess a distorted octahedral coordination geometry in which Ni(II) is coordinated to four nitrogen atoms of the tetradentate ligands and two CH_3CN (**2**, **3**, **4**) or one H_2O and one CH_3CN (**1a**) are located in *cis* positions. The $Ni–N_{py}$ bond distances (2.054(2)–2.078(3) Å) in **1a**, **2** and **3** are shorter than the $Ni–N_{amine}$ bonds (2.127(2)–2.196(3) Å) because of sp^2 and sp^3 hybridizations of the pyridyl and tertiary amine nitrogens respectively. In **3** the $Ni–N_{im}$ bond (2.040(5) Å) is shorter than the $Ni–N_{py}$ bond (2.074(4) Å) due to the stronger coordination of imidazole compared with the pyridine donor. In dichloromethane/acetonitrile solvent mixture, all the Ni(II) complexes possess an octahedral coordination geometry, as revealed by the characteristic ligand field bands in the visible region. They efficiently catalyze the hydroxylation of alkanes when *m*-CPBA is used as oxidant with turnover number (TON) in the range of 340–620 and good alcohol selectivity for cyclohexane (A/K, 5–9). By replacing one of the pyridyl donors in TPA by a weakly coordinating $–NMe_2$ or $–NEt_2$ donor nitrogen atom the catalytic activity decreases slightly with no change in the selectivity. In contrast, upon replacing the pyridyl nitrogen donor by the strongly σ-bonding imidazolyl or sterically demanding quinolyl/benzimidazolyl nitrogen donor, both the catalytic activity and selectivity decrease, possibly due to destabilization of the intermediate $[(4N)(CH_3CN)Ni–O^{\bullet}]^+$ radical species. Adamantane is selectively (3°/2°, 12–17) oxidized to 1-adamantanol, 2-adamantanol and 2-adamantanone while cumene is selectively oxidized to 2-phenyl-2-propanol. In contrast to cyclohexane oxidation, the incorporation of sterically hindering quinolyl/benzimidazolyl donors around Ni(II) leads to a high 3°/2° bond selectivity for adamantane oxidation. A linear correlation between the metal–ligand covalency parameter (β) and the turnover number has been observed.

Introduction

In Nature a variety of biologically essential transformations are catalyzed by iron containing enzymes such as methane monooxygenases, cytochrome P450 and bleomycin. In particular, the soluble methane monooxygenases (sMMO) are widely investigated metalloenzymes that catalyze the oxidation of methane to methanol using dioxygen.[1–10] Inspired by these enzymes, significant efforts have been made to reproduce the functional aspects of the non-heme diiron enzymes by designing model complexes, which are attractive as they catalyze unique selective chemical transformations such as methane oxidation using dioxygen or peroxide. Several bio-inspired iron(II)/(III) complexes have been investigated as catalysts for hydroxylation, epoxidation and sulfoxidation reactions.[11–24] In recent years catalytic oxidation

[a]*Centre for Bioinorganic Chemistry, School of Chemistry, Bharathidasan University, Tiruchirappalli, 620 024, Tamil Nadu, India. E-mail: palanim51@yahoo.com, palaniandavarm@gmail.com*
[b]*Analytical Science Discipline, Central Salt and Marine Chemicals Research Institute, Bhavnagar, 364 002, India*

† CCDC reference numbers 805447–805450. For crystallographic data in CIF or other electronic format see DOI: 10.1039/c1dt10902b

of saturated hydrocarbons under mild conditions has become an exciting and challenging scientific goal and has received greater attention.[25–30] Though iron complexes are considered to be one of the most promising catalysts for this industrially important reaction, a variety of metal-based homogeneous catalysts for alkane oxidation have been reported by replacing iron with different transition metals such as Mn, Co, Cu, Ru and Os.[31–51] Among them, ruthenium has attracted much attention and a few Ru(II/III) complexes of tripodal 4N ligands based on tris(2-pyridylmethyl)amine (TPA)[52] and tris(benzimidazol-2-ylmethyl)amine (NTB)[53] have been studied as catalysts for alkane hydroxylation, and the involvement of a Ru^{V}═O intermediate in the catalytic cycle has been proposed.

Recently, nickel has attracted regarding catalysts for the hydroxylation of alkanes in view of its industrial importance. Earlier several oxo-bridged dinuclear Ni(II) complexes have been reported to be involved in oxygen activation chemistry.[54–66] Very recently, Itoh *et al.* have demonstrated[67] that the Ni(II) complex [Ni(TPA)(OAc)(H_2O)](BPh_4) is a very efficient and robust turnover catalyst showing a high alcohol selectivity for alkane hydroxylation with *m*-chloroperbenzoic acid (*m*-CPBA) as oxidant. Later, they isolated a series of Ni(II) complexes of 3N, tripodal 4N and 3NO ligands and studied the effect of ligand and counter anion on the catalytic oxidation of cyclohexane with *m*-CPBA, suggesting the involvement of the highly reactive nickel-oxo (Ni═O^{+}) intermediate rather than an auto-oxidation type free radical species in the catalytic cycle.[68] Also, the same group reported Ni(II) complexes of tripodal phenolate ligands, which are capable of catalyzing the oxidation of cyclohexane to cyclohexanol using *m*-CPBA with up to 100% conversion based on the oxidant in solvent free conditions.[69] Also, Hikichi *et al.* crystallized the nickel(II) alkylperoxo complex [Ni^{II}(Tp^{ipr})(OO*t*Bu)] and studied its oxidation activity towards substituted benzaldehydes.[70] However, the factors determining the selectivity as well as efficiency of the catalysts and the nature of intermediate species still remain unclear.

All the above observations prompted us to isolate Ni(II) complexes of systematically varied tripodal 4N ligands containing pyridine, imidazole, sterically demanding quinoline and benzimidazole moieties and weakly binding –NMe_2/–NEt_2 groups, and study the influence of the ligand stereoelectronic factors upon the efficiency as well as the alcohol product selectivity of the complexes as catalysts for alkane hydroxylation reactions. We aim to construct more efficient and alcohol selective catalysts for alkane hydroxylation and also collect evidence for the reactive intermediate involved in the alkane hydroxylation reaction. All the present nickel(II) complexes catalyse the hydroxylation of alkanes such as cyclohexane, adamantane, ethylbenzene and cumene efficiently with good alcohol selectivity using *m*-CPBA as the oxidant within two hours. Also, upon increasing the concentration of substrate the TON reaches 730 with a slight increase in the A/K ratio (9.0). Furthermore, when the pyridine moiety in the Ni(II) catalyst is replaced with the strongly σ-bonding (benz)imidazolyl moiety both the efficiency and selectivity of the catalyst decrease, and when a –NMe_2 donor group is replaced with a weakly σ-bonding –NEt_2 donor group the selectivity of the catalyst remains approximately the same. In contrast, for adamantane oxidation the incorporation of sterically hindering quinolyl/benzimidazolyl donors around Ni(II) leads to a high 3°/2° bond selectivity.

Experimental

Materials

Pyridine-2-carboxaldehyde, 2-aminomethylpyridine, *N*,*N*-dimethylethylenediamine, *N*,*N*-diethylethylenediamine, sodium triacetoxyborohydride, sodium borohydride, 1-methyl-imidazole-2-carboxaldehyde, nickel(II) perchlorate hexahydrate, adamantane, cumene, sodium tetraphenylborate, *m*-choloroperbenzoic acid (Aldrich), quinoline-2-carboxaldehyde (Alfa Aesar), acetic acid glacial, dichloromethane, diethylether (Merck, India), ethylbenzene, nitrilotriacetic acid, *o*-phenylenediamine (Loba, India) and cyclohexane (Ranbaxy) were used as received. Methanol (Sisco Research Laboratory, Mumbai), acetonitrile and tetrahydrofuran (Merck, India) were distilled before use.

Synthesis of ligands

***N*,*N*-Dimethyl-*N*′,*N*′-bis(pyrid-2-ylmethyl)ethane-1,2-diamine (L1).** The ligand was prepared as reported[71] elsewhere. Yield: 1.19 g (88%). ^{1}H NMR (400 MHz, $CDCl_3$): δ 2.18 (s, 6H), 2.41 (t, 2H), 2.65 (t, 2H), 3.87 (s, 4H), 7.15 (t, 2H), 7.53 (d, 2H), 7.65 (t, 2H), 8.51 (d, 2H). EI-MS *m*/*z* = 270.1 $C_{16}H_{22}N_4^{\bullet+}$.

***N*,*N*-Diethyl-*N*′,*N*′-bis(pyrid-2-ylmethyl)ethane-1,2-diamine (L2).** The procedure employed for **L1** was used for the preparation of **L2**. *N*,*N*-Diethylethylenediamine was used in the place of *N*,*N*-dimethylethylenediamine. The pale yellow oil formed was used without further purification for complex preparation. Yield: 1.38 g (92%). ^{1}H NMR (400 MHz, $CDCl_3$): δ 1.12 (t, 6H), 2.28 (q, 4H), 2.49 (t, 2H), 2.58 (t, 2H), 3.83 (s, 4H), 7.18 (t, 2H), 7.49 (d, 2H), 7.68 (t, 2H), 8.61 (d, 2H). EI-MS *m*/*z* = 298.21 $C_{18}H_{26}N_4^{\bullet+}$.

***N*,*N*-Dimethyl-*N*′-(1-methyl-*1H*-imidazol-2-ylmethyl)-*N*′-(pyrid-2-ylmethyl)ethane-1,2-diamine (L3).** *N*,*N*-dimethyl-*N*′-(pyrid-2-ylmethyl)ethane-1,2-diamine was prepared as reported[72] and the reductive amination of this compound with 1-methylimidazole-2-carboxaldehyde using sodium triacetoxyborohydride gave **L3** as a pale yellow oil, which was used without further purification for the isolation of the complex. Yield: 1.12 g (82%). ^{1}H NMR (400 MHz, $CDCl_3$): δ 2.13 (s, 6H), 2.44 (t, 2H), 2.63 (t, 2H), 3.67 (s, 3H), 3.58 (s, 2H), 3.78 (s, 2H), 6.78 (s, 1H), 6.86 (s, 1H), 7.17 (t, 1H), 7.46 (d, 1H), 7.63 (t, 1H), 8.58 (d, 1H). EI-MS *m*/*z* = 273.2 $C_{15}H_{23}N_5^{\bullet+}$.

***N*,*N*-Dimethyl-*N*′,*N*′-bis(1-methyl-*1H*-imidazol-2-ylmethyl)-ethane-1,2-diamine (L4).** The procedure employed for the preparation of **L1** was also used for **L4** and 1-methylimidazole-2-carboxaldehyde was used instead of pyridine-2-carboxaldehyde. The colorless oil was used without further purification for complex preparation. Yield: 1.05 g (76%). ^{1}H NMR (400 MHz, $CDCl_3$): δ 2.14 (s, 6H), 2.41 (t, 2H), 2.59 (t, 2H), 3.68 (s, 6H), 3.59 (s, 4H), 6.80 (s, 2H), 6.87 (s, 2H). EI-MS *m*/*z* = 276.2 $C_{14}H_{24}N_6^{\bullet+}$.

***N*,*N*-Dimethyl-*N*′,*N*′-bis(quinolin-2-ylmethyl)ethane-1,2-diamine (L5).** The procedure employed for the preparation of **L1** was also used for **L5** and quinoline-2-carboxaldehyde was used instead of pyridine-2-carboxaldehyde. The brown oil was used without further purification for the isolation of the complex. Yield: 1.28 g (69%). ^{1}H NMR (400 MHz, $CDCl_3$): δ 2.13 (s, 6H), 2.42 (t, 2H), 2.62 (t, 2H), 3.80 (s, 4H), 7.15 (d, 2H), 7.42 (t, 2H), 7.57 (t,

2H), 7.67 (d, 2H), 7.89 (d, 2H), 8.13 (d, 2H). EI-MS m/z = 370.2 $C_{24}H_{26}N_4^{\bullet+}$.

Tris(benzimidazol-2-ylmethyl)amine (L6). This ligand was prepared as reported elsewhere.[73] The ^{1}H NMR data agreed well with that reported.

Tris(pyrid-2ylmethyl)amine (L7). The ligand was prepared as reported earlier.[71] Yield: 1.27 g (87%). ^{1}H NMR (400 MHz, $CDCl_3$): δ 3.85 (s, 6H), 7.16 (t, 3H), 7.49 (d, 3H), 7.72 (t, 3H), 8.54 (d, 3H). EI-MS m/z = 290.1 $C_{18}H_{18}N_4^{\bullet+}$.

Synthesis of Ni(II) complexes

[Ni(L1)(H$_2$O)(CH$_3$CN)](ClO$_4$)$_2$ 1a. A methanol solution (5 mL) of $Ni(ClO_4)_2{\cdot}6H_2O$ (0.365 g, 1 mmol) was added to **L1** (0.27 g, 1 mmol) in methanol solution (5 mL) with stirring at room temperature. The colour of the solution turned to indigo. After stirring the solution for 30 min, 5 mL of acetonitrile was added. The solution was stirred for an additional 30 min and the color of the solution turned to blue. Ether diffusion of the blue coloured solution gave blue crystals, which were suitable for X-ray crystallographic analysis. Yield, 0.51 g, 87%. FT-IR (KBr) 3411 (b), 2998 (b), 2265 (s), 1591 (s), 1468 (s), 1439 (s), 1378 (s), 1349 (s), 1093 (s), 764 (s), 625 (s) cm^{-1}. ESI-MS: m/z 184.52 [(M–CH_3CN–2BPh$_4$)$^{2+}$]. Anal. Calcd. $C_{18}H_{27}N_5O_9Cl_2Ni$: C, 36.83; H, 4.64; N, 11.93. Found: C, 36.75; H, 4.50; N, 11.79.

[Ni(L1)(CH$_3$CN)$_2$](BPh$_4$)$_2$ 1. This was obtained from the metathesis of **1a** by adding $NaBPh_4$ (0.684 g, 2 mmol) in methanol. The pink precipitate was filtered off, washed with small quantities of ice-cold methanol and then dried. Yield, 0.87 g, 83%. FT-IR (KBr) 3435 (b), 2265 (s), 1593 (s), 1476 (s), 1382 (s), 1350 (s), 1100 (s), 735 (s), 707 (s), 608 (s) cm^{-1}. ESI-MS: m/z 184.47 [(M–CH_3CN–2BPh$_4$)$^{2+}$]. Anal. Calcd. $C_{68}H_{68}N_6B_2Ni$: C, 77.81; H, 6.53; N, 8.01. Found: C, 77.89; H, 6.61; N, 7.94.

The complexes **2–7** were prepared by using the procedure employed for isolating **1** and using the ligands **L2–L7**.

[Ni(L2)(CH$_3$CN)$_2$](BPh$_4$)$_2{\cdot}$CH$_3$CN 2. Yield, 0.95 g, 85%. FT-IR (KBr) 3457 (b), 3043 (s), 2268 (s), 1606 (s), 1479 (s), 1443 (s), 1425 (s), 1382 (s), 1350 (s), 1097 (s), 735 (s), 705 (s), 610 (s) cm^{-1}. ESI-MS: m/z 198.51 [(M–CH_3CN–2BPh$_4$)$^{2+}$]. Anal. Calcd. for $C_{72}H_{75}N_7B_2Ni$: C, 77.30; H, 6.76; N, 8.76. Found: C, 77.20; H, 6.68; N, 8.71. Single crystals suitable for X-ray crystallographic analysis were obtained by slow evaporation of a CH_3CN/DCM solution of the complex.

[Ni(L3)(CH$_3$CN)$_2$](BPh$_4$)$_2$ 3. Yield 0.79 g, 76%. FT-IR (KBr) 3470 (b), 2265 (s), 1606 (s), 1511 (s), 1475 (s), 1418 (s), 1382 (s), 1350 (s), 1125 (s), 1105 (s), 1030 (s), 978 (s), 842 (s), 818 (s), 734 (s), 707 (s), 610 (s) cm^{-1}. ESI-MS: m/z 185.90 [(M–CH_3CN–2BPh$_4$)$^{2+}$]. Anal. Calcd. for $C_{67}H_{69}N_7B_2Ni$: C, 76.45; H, 6.61; N, 9.31. Found: C, 76.37; H, 6.68; N, 9.23. Single crystals suitable for X-ray crystallographic analysis were obtained by slow evaporation of a CH_3CN/DCM solution of the complex.

[Ni(L4)(CH$_3$CN)$_2$](BPh$_4$)$_2{\cdot}$CH$_3$CN 4. Yield 0.78 g, 71%. FT-IR (KBr) 3497 (b), 3050 (s), 2268 (s), 1607 (s), 1505 (s), 1472 (s), 1421 (s), 1382 (s), 1349 (s), 1129 (s), 1105 (s), 1031 (s), 982 (s), 843 (s), 818 (s), 731 (s), 708 (s), 611 (s) cm^{-1}. ESI-MS: m/z 187.50 [(M–2CH_3CN–2BPh$_4$)$^{2+}$]. Anal. Calcd. for $C_{68}H_{73}N_9B_2Ni$: C, 74.47; H, 6.71; N, 11.49. Found: C, 74.39; H, 6.74; N, 11.45. Single crystals suitable for X-ray crystallographic analysis were obtained by slow evaporation of a CH_3CN/DCM solution of the complex.

[Ni(L5)(CH$_3$CN)$_2$](BPh$_4$)$_2$ 5. Yield 0.80 g, 70%. FT-IR (KBr): 3410 (b), 2266 (s), 1595 (s), 1512 (s), 1476 (s), 1425 (s), 1382 (s), 1346 (s), 1143 (s), 1125 (s), 1028 (s), 948 (s), 731 (s), 705 (s), 608 (s) cm^{-1}. ESI-MS: m/z 234.48 [(M–CH_3CN–2BPh$_4$)$^{2+}$]. Anal. Calcd. for $C_{76}H_{72}N_6B_2Ni$: C, 79.39; H, 6.31; N, 7.31. Found: C, 79.28; H, 6.28; N, 7.20.

[Ni(L6)(CH$_3$CN)$_2$](BPh$_4$)$_2$ 6. Yield 0.94 g, 79%. FT-IR (KBr) 3385 (b), 2804 (b), 2265 (s), 1590 (s), 1450 (s), 1385 (s), 1346 (s), 1143 (s), 1111 (s), 1090 (s), 739 (s), 705 (s), 623 (s) cm^{-1}. ESI-MS: m/z 252.95 [(M–CH_3CN–2BPh$_4$)$^{2+}$]. Anal. Calcd. for $C_{76}H_{67}N_9B_2Ni$: C, 76.92; H, 5.69; N, 10.62. Found: C, 76.87; H, 5.61; N, 10.54.

[Ni(L7)(CH$_3$CN)$_2$](BPh$_4$)$_2$ 7. Yield 0.89 g, 82%. FT-IR (KBr) 2265 (s), 1595 (s), 735 (s), 707 (s) cm^{-1}. ESI-MS: m/z 194.49 [(M-CH_3CN–2BPh$_4$)$^{2+}$]. Anal. Calcd. for $C_{71}H_{68}N_6B_2Ni$: C, 78.55; H, 6.31; N, 7.74. Found: C, 78.48; H, 6.37; N, 7.70.

Caution: Perchlorate salts of the compounds are potentially explosive. Only small quantities of these compounds should be prepared and suitable precautions should be taken when they are handled.

Catalytic oxidations

The oxidation of alkanes was carried out at room temperature under research grade nitrogen atmosphere. In a typical reaction, Ni(II) complex (0.35×10^{-3} mmol dm^{-3}) was added to a mixture of alkanes (2.45 mol dm^{-3}) and oxidant *m*-CPBA (0.35 mol dm^{-3}) in CH_2Cl_2 : CH_3CN mixture (3 : 1 v/v). After 1 h the reaction mixture was quenched with triphenylphosphine, the reaction mixture was filtered over a silica column and then eluted with diethylether. An internal standard (bromobenzene) was added at this point and the solution was subjected to GC analysis. The mixture of organic products was identified by Agilent GC-MS and quantitatively analyzed by HP 6890 series GC equipped with HP-5 capillary column (30 m × 0.32 mm × 2.5 μm) using a calibration curve obtained with authentic compounds. All of the products were quantified using GC (FID) with the following temperature program: injector temperature 130 °C; initial temperature 60 °C, heating rate 10 °C min^{-1} to 130 °C, increasing the temperature to 160 °C at a rate of 2 °C min^{-1}, and then increasing the temperature to 260 °C at a rate of 5 °C min^{-1}; FID temperature 280 °C. GC-MS analysis was performed under conditions identical to those used for GC analysis. The average of three measurements are reported.

Physical measurements

Elemental analyses were performed on a Perkin Elmer Series II CHNS/O analyzer 2400. The electronic spectra were recorded on an Agilent 8453 diode array spectrophotometer. ^{1}H NMR spectra were recorded on a Bruker 400 MHz NMR spectrometer. ESI-MS analysis were recorded on a Micromass Quattro II triple quadrupole mass spectrometer. IR spectra were recorded on a Perkin Elmer FT-IR spectrometer. GC-MS analysis was performed on an Agilent GC-MS equipped with 7890A GC series (HP-5 capillary column) and 5975C inert MSD. The

Table 1 Crystallographic data for **1a**, **2**, **3** and **4**

	1a	**2**	**3**	**4**
Empirical formula	$C_{18}H_{27}N_5Cl_2O_9Ni$	$C_{72}H_{72}B_2N_7Ni$	$C_{134}H_{138}B_4N_{14}Ni_2$	$C_{68}H_{73}B_2N_9Ni$
Formula weight/g mol^{-1}	587.06	1115.70	2105.24	1096.68
Crystal habit, colour	Purple	Pink	Pink	Violet
Crystal system	Monoclinic	Monoclinic	Monoclinic	Monoclinic
Crystal size	0.53 × 0.26 × 0.13 mm	0.39 × 0.37 × 0.21 mm	0.60 × 0.48 × 0.38 mm	0.20 × 0.15 × 0.13 mm
Space group	P21/c	P 21/c	P21/c	P21/c
a/Å	15.8006(12)	20.1135(16)	19.4952(12)	10.9038(2)
b/Å	10.4718(8)	13.4486(11)	17.3430(10)	14.9757(2)
c/Å	15.1299(11)	23.7510(19)	34.986(2)	37.0413(6)
α (°)	90.000	90.000	90.000	90.000
β (°)	106.9420(10)	110.286(2)	92.5370(10)	90.7660(10)
γ (°)	90	90	90	90
V/Å^3	2394.8(3)	6026.1(8)	11817.2(12)	6048.01(17)
Z	4	4	4	4
ρ_c/g cm^{-3}	1.628	1.230	1.183	1.204
F(000)	1216.0	2364.0	4464.0	2328.0
T/K	100	100	293	293
No. of Reflections collected	14152	11414	20794	14067
No. of unique reflections	5595	5848	12409	8622
Radiation (Mo-Kα)/Å	0.71073	0.71073	0.71073	0.71073
Goodness-of-fit on F^2	1.051	0.836	1.074	1.014
Number of refined Parameters	327	732	1397	728
R_1/w $R2[I > 2\sigma(I)]^a$	0.0481/0.1126	0.0662/0.1157	0.0879/0.1758	0.0489/0.1022
R_1/w R_2 (all data)	0.0558/0.1171	0.1342/0.1342	0.1507/0.2019	0.1043/0.1227

^{a} $R1 = [\Sigma(\|F_o\| - \|F_c\|)/\Sigma|F_o|]$; $wR2 = \{[\Sigma(w(F_o^2 - F_c^2)^2)/\Sigma(wF_o^4)]^{1/2}\}$

products were quantified by using Hewlett Packard (HP) 6890 Gas Chromatograph (GC) series equipped with a FID detector and a HP-5 capillary column (30 m × 0.32 mm × 2.5 μm). All the catalytic reactions were performed under a research grade nitrogen atmosphere using standard Schlenk line techniques.

Crystal data collection and structure refinement

The diffraction experiments were carried out on a Bruker SMART APEX diffractometer equipped with a CCD area detector. High quality crystals, suitable for X-ray diffraction were chosen after careful examination under an optical microscope. Intensity data for the crystals were collected using Mo-Kα (λ = 0.71073 Å) radiation on a Bruker SMART APEX diffractometer equipped with CCD area detector at 100 and 293 K. The data integration and reduction was processed with SAINT[74] software. An empirical absorption correction was applied to the collected reflections with SADABS.[75] The structures were solved by direct methods using SHELXTL[76] and refined on F^2 by the full-matrix least-squares technique using the SHELXL-97[77] package. Even though the data of **2** was collected at liquid nitrogen temperature (100 K), during the structure solution it was observed that the carbon atoms of the coordinated acetonitrile molecule in **2** appeared as diffused peaks and the methyl carbon is disordered. Both these carbon atoms were located from the difference Fourier map, and since the peak heights of the carbon atoms were small and diffused the whole coordinated CH_3CN molecule was refined only isotropically. For the disordered methyl carbon the occupancy factor is assigned using FVAR command. Crystal data and additional details of the data collection and refinement of the structure are presented in Table 1. The selected bond lengths and bond angles are listed in Table 2.

Table 2 Selected bond lengths [Å] and bond angles [°] for **1a** and **2**

1a		**2**	
Bond lengths/Å			
Ni(1)–N(1)	2.054(2)	Ni(1)–N(1)	2.069(3)
Ni(1)–N(2)	2.090(2)	Ni(1)–N(2)	2.079(3)
Ni(1)–N(3)	2.088(2)	Ni(1)–N(3)	2.078(3)
Ni(1)–N(4)	2.127(2)	Ni(1)–N(4)	2.196(3)
Ni(1)–N(5)	2.044(2)	Ni(1)–N(5)	2.170(3)
Ni(1)–O(9)	2.154(2)	Ni(1)–N(6)	2.031(4)
Bond angles/°			
N(5)–Ni(1)– N(1)	100.34(9)	N(6)–Ni(1)–N(1)	97.12
N(5)–Ni(1)–N(3)	97.17(9)	N(6)–Ni(1)–N(3)	98.43(14)
N(1)–Ni(1)–N(3)	159.57(9)	N(1)–Ni(1)–N(3)	160.05(13)
N(5)–Ni(1)–N(2)	176.39(9)	N(6)–Ni(1)–N(2)	179.11(13)
N(1)–Ni(1)–N(2)	82.18(9)	N(1)–Ni(1)–N(2)	82.46(13)
N(3)–Ni(1)–N(2)	80.85(9)	N(3)–Ni(1)–N(2)	81.80(13)
N(5)–Ni(1)–N(4)	91.62(9)	N(6)–Ni(1)–N(5)	88.49(13)
N(1)–Ni(1)–N(4)	92.72(9)	N(1)–Ni(1)–N(5)	84.63(12)
N(3)–Ni(1)–N(4)	97.25(9)	N(3)–Ni(1)–N(5)	83.36(12)
N(2)–Ni(1)–N(4)	85.65(9)	N(2)–Ni(1)–N(5)	90.69(12)
N(5)–Ni(1)–O(9)	84.67(9)	N(6)–Ni(1)–N(4)	95.98(13)
N(1)–Ni(1)–O(9)	84.92(9)	N(1)–Ni(1)–N(4)	92.26(12)
N(3)–Ni(1)–O(9)	86.32(9)	N(3)–Ni(1)–N(4)	98.45(12)
N(2)–Ni(1)–O(9)	98.18(9)	N(2)–Ni(1)–N(4)	84.83(12)
N(4)–Ni(1)–O(9)	175.16(9)	N(5)–Ni(1)–N(4)	174.86(13)

Results and discussion

Syntheses and characterization of ligands and their nickel(II) complexes

The tripodal tetradentate 4N ligands **L1–L7** (Scheme 1) were synthesized according to known procedures, which involve Schiff base condensation, reductive amination and fusion reaction. The ligands **L1**, **L2**, **L4**, **L5** and **L7** were prepared by reductive amination of *N*,*N*-dimethylethylenediamine/*N*,*N*-diethylethylenediamine with two

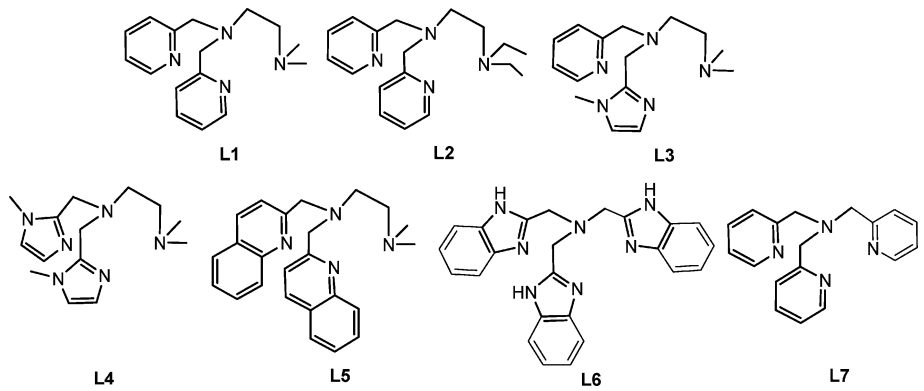

Scheme 1 Structures of 4N ligands employed in the study.

moles of pyridine-2-carboxaldehyde (**L1**, **L2**)/1-methylimidazole-2-carboxaldehyde (**L4**)/quinoline-2-carboxaldehyde (**L5**) using sodium triacetoxyborohydride as reducing agent and were characterized by ^{1}H NMR spectroscopy and mass spectrometry. The ligand **L3** was prepared by Schiff base condensation of *N*,*N*-dimethylethylenediamine with pyridine-2-carboxaldehyde, followed by reduction and then reductive amination with 1-methylimidazole-2-carboxaldehyde. The ligand **L6** was prepared by fusing nitrilotriacetic acid with *o*-phenylenediamine as previously reported.[73] The nickel(II) complex **1a** was isolated by treating **L1** with $Ni(ClO_4)_2{\cdot}6H_2O$ in methanol and then adding acetonitrile. The nickel(II) complexes $[Ni(L)(CH_3CN)_2](BPh_4)_2$ **1–7** were isolated by treating $Ni(ClO_4)_2{\cdot}6H_2O$ with the corresponding ligands **L1–L7** in methanol, adding acetonitrile with stirring and then treating the reaction mixture with stoichiometric amounts of $NaBPh_4$. All the complexes were characterized by using elemental analysis and electronic spectroscopy. The formulation of the complexes based on elemental analysis was confirmed by determining the X-ray crystal structures of **1a**, **2**, **3** and **4**. The tripodal ligands with different electron-releasing abilities are expected to play an important role in determining the stability of the intermediate involved in the catalytic cycle and hence the reactivity.

Description of X-ray crystal structures of $[Ni(L1)(H_2O)(CH_3CN)](ClO_4)_2$ 1a, $[Ni(L2)(CH_3CN)_2](BPh_4)_2$ 2, $[Ni(L3)(CH_3CN)_2](BPh_4)_2$ 3 and $[Ni(L4)(CH_3CN)_2](BPh_4)_2$ 4

The molecular structure of $[Ni(L1)(H_2O)(CH_3CN)](ClO_4)_2$ **1a** is shown in Fig. 1 together with the atom numbering scheme and the selected bond lengths and bond angles are collected in Table 2. The complex contains a NiN_5O coordination sphere with a distorted octahedral coordination geometry constituted by two pyridine and two tertiary amine nitrogen atoms of the tripodal ligand **L1**, and the remaining two *cis*-coordination sites *trans* to the tertiary amine nitrogen atoms are occupied by water and acetonitrile molecules. The Ni–N_{py} bonds (2.054(2), 2.088(2) Å) are shorter than the Ni–N_{amine} bonds (2.090(2), 2.127(2) Å) due to sp^2 and sp^3 hybridizations of the pyridyl and tertiary amine nitrogen atoms respectively. Also, the terminal Ni–$N4_{amine}$ bond (2.127(2) Å) is longer than the Ni–$N2_{amine}$ bond (2.090(2) Å) formed by the apical amine nitrogen atom of the tripodal ligand, as expected. Furthermore, the coordination geometry of the complex cation

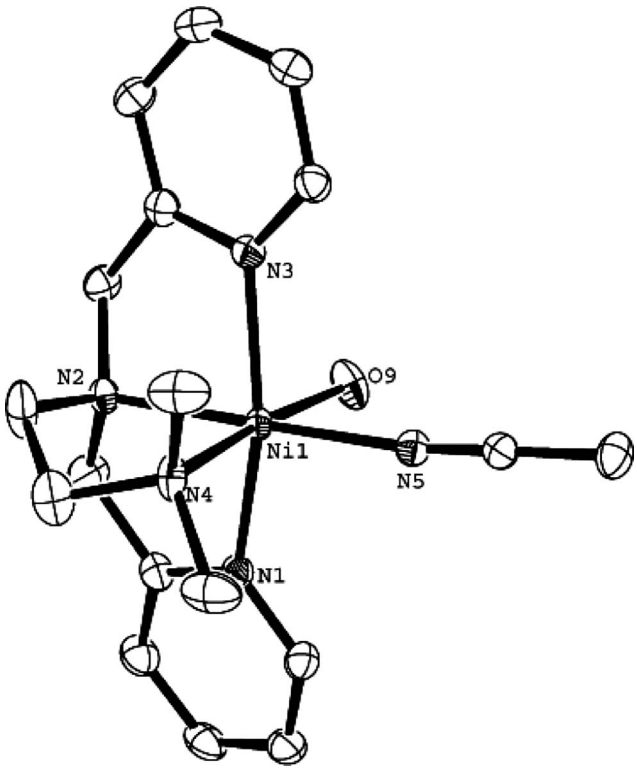

Fig. 1 Molecular structure of the $[Ni(L1)(H_2O)(CH_3CN)]^{2+}$ **1a** (50% probability factor for the thermal ellipsoid). Hydrogen atoms have been omitted for clarity.

is very similar to that of $[Ni(TPA)(OAc)(H_2O)]^+$ in which TPA occupies four sites of the octahedron and a water molecule and acetate ion occupy the remaining two sites.[69] Also, the Ni–N_{py}, Ni–N_{amine} and Ni–O bond distances in **1a** are similar to those observed for the nickel(II) complex cation $[Ni(TPA)(OAc)(H_2O)]^+$.

The X-ray crystal structures of $[Ni(L2)(CH_3CN)_2]^{2+}$ **2**, $[Ni(L3)(CH_3CN)_2]^{2+}$ **3** and $[Ni(L4)(CH_3CN)_2]^{2+}$ **4** are shown in Fig. 2, 3 and 4 respectively together with the atom numbering scheme, and the selected bond lengths and bond angles are collected in Table 2 and 3. The distorted octahedral coordination geometry of **2** is similar to that of **1a**. While the two pyridine and two tertiary amine nitrogen atoms of **L2** occupy the four coordination sites of the octahedron in **2**, the acetonitrile molecules occupy the remaining two *cis*-coordination sites. The Ni–NEt_2

Table 3 Selected bond lengths [Å] and bond angles [°] for **3** and **4**

3		**4**	
Ni(1)–N(1)	2.040(5)	Ni(1)–N(1)	2.079(2)
Ni(1)–N(3)	2.102(4)	Ni(1)–N(3)	2.133(16)
Ni(1)–N(4)	2.074(4)	Ni(1)–N(4)	2.0376(19)
Ni(1)–N(5)	2.148(4)	Ni(1)–N(6)	2.1481(18)
Ni(1)–N(6)	2.036(4)	Ni(1)–N(7)	2.062(2)
Ni(1)–N(7)	2.167(5)	Ni(1)–N(8)	2.0735(19)
Ni(2)–N(8)	2.058(4)		
Ni(2)–N(10)	2.108(4)		
Ni(2)–N(11)	2.073(4)		
Ni(2)–N(12)	2.148(4)		
Ni(2)–N(13)	2.167(5)		
Ni(2)–N(14)	2.065(4)		
Bond angles/°			
N(6)–Ni(1)–N(1)	98.68(19)	N(4)–Ni(1)–N(8)	99.09(8)
N(6)–Ni(1)–N(4)	98.99(18)	N(4)–Ni(1)–N(1)	157.51(7)
N(1)–Ni(1)–N(4)	159.8(2)	N(8)–Ni(1)–N(1)	101.30(8)
N(6)–Ni(1)–N(3)	176.88(18)	N(4)–Ni(1)–N(3)	81.67(7)
N(1)–Ni(1)–N(3)	82.4(2)	N(8)–Ni(1)–N(3)	176.12(7)
N(4)–Ni(1)–N(3)	80.5(2)	N(1)–Ni(1)–N(3)	78.64(7)
N(6)–Ni(1)–N(5)	92.11(17)	N(4)–Ni(1)–N(6)	91.77(7)
N(1)–Ni(1)–N(5)	92.90(18)	N(8)–Ni(1)–N(6)	91.23(8)
N(4)–Ni(1)–N(5)	96.22(18)	N(1)–Ni(1)–N(6)	97.17(8)
N(3)–Ni(1)–N(5)	84.89(18)	N(3)–Ni(1)–N(6)	84.94(7)
N(6)–Ni(1)–N(7)	91.54(16)	N(4)–Ni(1)–N(7)	88.43(8)
N(1)–Ni(1)–N(7)	86.58(17)	N(8)–Ni(1)–N(7)	87.49(8)
N(4)–Ni(1)–N(7)	83.17(17)	N(1)–Ni(1)–N(7)	83.09(8)
N(3)–Ni(1)–N(7)	91.46(18)	N(3)–Ni(1)–N(7)	96.34(7)
N(5)–Ni(1)–N(7)	176.35(16)	N(6)–Ni(1)–N(7)	178.72(7)
N(8)–Ni(2)–N(14)	101.52(17)		
N(8)–Ni(2)–N(11)	158.71(17)		
N(14)–Ni(2)–N(11)	97.56(18)		
N(8)–Ni(2)–N(10)	80.21(16)		
N(14)–Ni(2)–N(10)	177.71(17)		
N(11)–Ni(2)–N(10)	80.99(16)		
N(8)–Ni(2)–N(12)	95.45(18)		
N(14)–Ni(2)–N(12)	92.19(17)		
N(11)–Ni(2)–N(12)	93.15(17)		
N(10)–Ni(2)–N(12)	86.14(18)		
N(8)–Ni(2)–N(13)	84.70(17)		
N(14)–Ni(2)–N(13)	91.10(16)		
N(11)–Ni(2)–N(13)	85.59(16)		
N(10)–Ni(2)–N)13)	90.55(17)		
N(12)–Ni(2)–N(13)	176.61(17)		

bond in **2** (2.196(3) Å) is longer than the Ni–NMe_2 bond in **1a** (2.127(2) Å), obviously due to the more sterically hindering –NEt_2 group forming a coordinate bond to the Ni(II) center that is weaker than that formed by the –NMe_2 group. In **3** there are two crystallographically independent complex molecules in the same asymmetric unit cell, which exhibit the same coordination geometry but slightly different bond lengths and bond angles. Each molecule in the unit cell possesses a distorted octahedral coordination geometry constituted by one pyridine, one imidazole and two tertiary amine nitrogen atoms of the tripodal ligand, and acetonitrile molecules occupy the *cis* positions as in **2**. In **3** the Ni–N_{im} bond (2.040(5) Å) is shorter than the Ni–N_{py} bond (2.074(4) Å) as the coordination of imidazole is stronger than that of the pyridine donor. The complex **4** possesses a distorted octahedral coordination geometry constituted by two imidazole and two tertiary amine nitrogen atoms of the tripodal ligand and acetonitrile molecules occupy the *cis* positions as in **2** and **3**. The Ni–NMe_2 bond distances in **3** (2.148(4) Å) and **4** (2.1481(18) Å) are longer than that in **1a** (2.127(2) Å) due to the replacement of pyridine nitrogen by the strongly σ-bonding

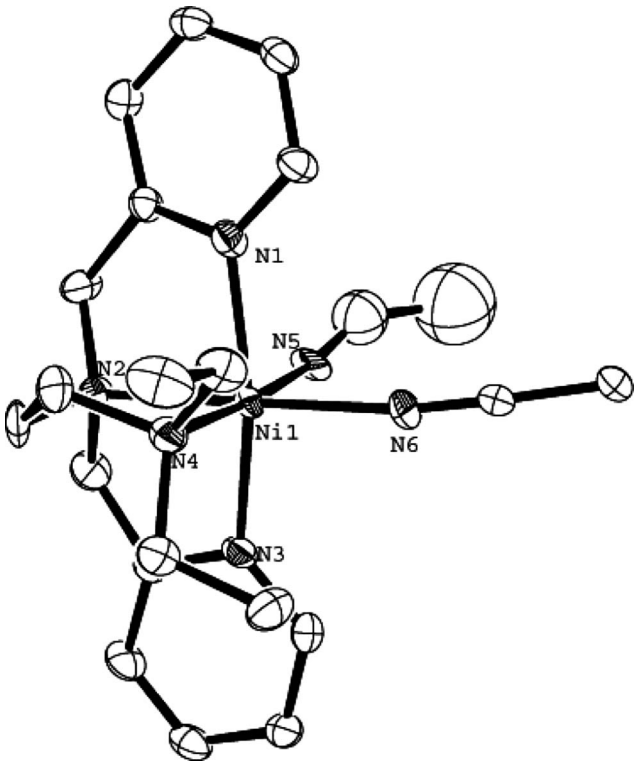

Fig. 2 Molecular structure of $[Ni(L2)(CH_3CN)_2]^{2+}$ **2** (50% probability factor for the thermal ellipsoid). Hydrogen atoms and lattice acetonitrile molecule have been omitted for clarity.

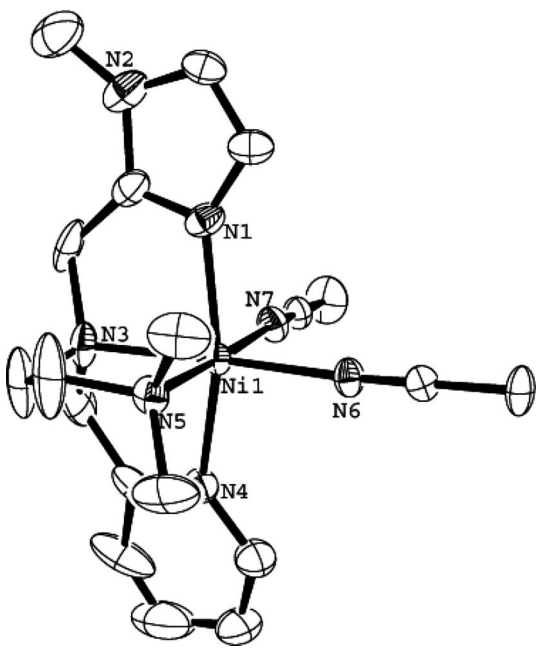

Fig. 3 Molecular structure of $[Ni(L3)(CH_3CN)_2]^{2+}$ **3** (20% probability factor for the thermal ellipsoid). Another molecule on the unit cell and hydrogen atoms have been omitted for clarity.

imidazole nitrogens. Similarly, the Ni–N_{amine} bond distance in **3** (2.102(4) Å) and **4** (2.133(16) Å) is longer than that in **1a** (2.090(2) Å) and **2** (2.079(3) Å) due to the stronger Ni–N_{ACN} (**3**: 2.036(4) Å; **4**: 2.062(2) Å) coordination. The Ni–N_{py} bond distances

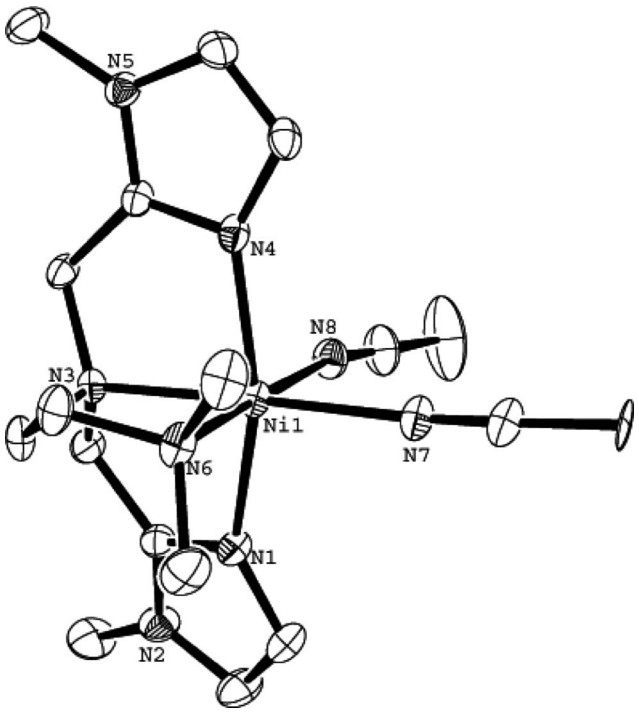

Fig. 4 Molecular structure of $[Ni(L4)(CH_3CN)_2]^{2+}$ **4** (20% probability factor for the thermal ellipsoid). Hydrogen atoms and lattice acetonitrile molecule have been omitted for clarity.

(2.069(3)–2.078(3) Å) in **2** and **3** are similar to those in **1a** and those in $[Ni(TPA)(OAc)(H_2O)]^+$ (2.057(6)–2.101(6) Å)[69] and are shorter than the Ni–N_{amine} bonds (2.079(3)–2.102(4) Å), as expected (*cf.* above). The terminal Ni–N_{amine} bonds (**2**: 2.196(3); **3**: 2.148(4) Å; **4**: 2.1481(18)) are longer than the central Ni–N_{amine} bonds (**2**: 2.079(3); **3**: 2.102(4) Å; **4**: 2.133(16) Å), as expected (*cf.* above).

For **1a**, **2**, **3** and **4** the N–Ni–N (78.64–101.52°) and N–Ni–N (157.51–179.11°) bond angles deviate from the ideal octahedral angles of 90° and 180° respectively revealing the presence of significant distortion in the Ni(II) coordination geometry.

Electronic spectral properties

The electronic spectral data of all the Ni(II) complexes are summarized in Table 4 and the typical electronic absorption spectrum of **1** is shown in Fig. 5. In a DCM : ACN (3 : 1 v/v) solvent mixture, all the present nickel(II) complexes exhibit two

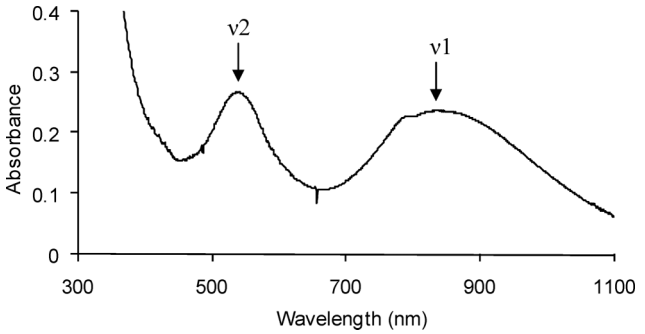

Fig. 5 Electronic absorption spectra of $[Ni(L2)(CH_3CN)_2](BPh_4)_2$ (1.0×10^{-2} M) in DCM:ACN (3 : 1 v/v) solvent mixture.

broad absorption bands in the ranges 540–570 and 840–980 nm together with a very weak shoulder in the range 770–800 nm. The lower energy band in the range 840–980 nm is assigned to $^3A_{2g} \rightarrow {}^3T_{2g}(F)$ (ν_1) transition, and the higher energy band in the range 540–570 nm to $^3A_{2g} \rightarrow {}^3T_{1g}(F)$ (ν_2) transition in Ni(II) located in an octahedral environment. The shoulder or band observed around 360 nm in the UV region is assigned to the $^3A_{2g} \rightarrow {}^3T_{1g}(P)$ (ν_3) transition while the weak shoulder in the range 770–800 nm to the $^3A_{2g} \rightarrow {}^1E_{1g}(D)$ spin-forbidden transition.[78] The observed ν_1 and ν_2 band positions are fitted into the quadratic equation[79] connecting the energies of both ν_1 and ν_3 transitions. The calculated band positions (ν_3) agree well with the observed ones (Table 4), which confirms the band assignments and hence the octahedral coordination geometry for Ni(II) in solution also. An analysis of values of the derived covalency parameter β[80,81] reveals interesting trends. A combination of two pyridyl nitrogen donors confers metal–ligand covalency higher than that of three pyridyl nitrogen donors bound to Ni(II) as in $[Ni(tpa)(CH_3CN)_2]^{2+}$ **7** indicating that the third pyridyl nitrogen located *cis* to the other two pyridyl nitrogens at a longer distance[67] is not effectively involved in π-back bonding. A combination of two pyridyl (**1**) or two imidazolyl (**4**) nitrogen donors confers a higher metal–ligand covalency than that of two quinolyl nitrogen donors (**5**) or that of one pyridyl and one imidazolyl donor (**3**), revealing that pyridyl nitrogen is better suited for π-back bonding. Also, a combination of three pyridyl donors leads to a higher covalency than that of three benzimidazolyl donors. The incorporation of σ-bonding $-NMe_2$/$-NEt_2$ donors also leads to a higher metal–ligand covalency. All these observations reveal that β may be taken as a measure of the metal–ligand π-back bonding in the complexes.

Table 4 UV-Visible spectral data (λ_{max} in nm; ε in M^{-1} cm^{-1} in parenthesis) of Ni(II) complexes **1–7** in DCM : ACN solvent mixture (1 : 3 v/v) at 25 °C

	$^3A_{2g} \rightarrow {}^3T_{1g}(P)$ (ν_3)						
Complex	Found	Calcd[a]	$^3A_{2g} \rightarrow {}^3T_{1g}(F)$ (ν_2)	$^3A_{2g} \rightarrow {}^1E_{1g}(D)$	$^3A_{2g} \rightarrow {}^3T_{2g}(F)$ (ν_1)	B″	[a] β (%)
1	—	342	540 (26)	788 (23)	840 (24)	801	26
1a	—	342	553 (30)	782 (13)	880 (18)	877	19
2	—	343	551 (31)	791 (20)	872 (26)	855	21
3	360 (75)	345	553 (37)	788 (10)	875 (30)	851	21
4	353 (90)	360	570 (40)	784 (11)	890 (26)	773	28
5	—	342	568 (45)	800 (12)	920 (30)	947	12
6	358 (120)	332	571 (40)	770 (10)	938 (24)	1038	4
7		331	533 (28)	785 (10)	845 (20)	893	17

[a] Calculated by solving the quadratic equation and using B as 1080 cm^{-1}

Table 5 Conversion of cyclohexane catalyzed[a] by **1** with time

Complex	Time (min)	Cyclohexane (TON)			Total TON[c]	A/K[d]	Yield[e] (%)
		-ol[b]	-one[b]	ε-caprolactone			
1	10	326	19	12	357	10.5	35.7
	30	475	22	28	525	9.5	52.5
	60	546	16	45	607	8.9	60.7
	120	558	12	52	622	8.7	62.2

[a] Reaction conditions: Catalyst (0.35×10^{-3} mmol dm^{-3}), Substrate (2.45 mol dm^{-3}), Oxidant (0.35 mol dm^{-3}) in DCM:ACN solvent mixture (3 : 1 v/v); [b] -ol = cyclohexanol and -one = cyclohexanone; [c] Total TON = no. of mmol of product/no. of mmol of catalyst; [d] A/K = TON of -ol/(TON of -one + TON of ε-caprolactone); [e] Yield based on the oxidant.

Table 6 Variation of substrate concentration for cyclohexane hydroxylation catalyzed[a] by **1**

Complex	Cyclohexane (mol dm^{-3})	Products (TON)			Total TON[c]	A/K[d]	Yield[e] (%)	Yield[f] (%)
		-ol[b]	-one[b]	ε-caprolactone				
1	0.35	93	18	38	149	1.6	14.9	14.9
	0.70	160	14	48	222	2.5	22.2	11.1
	1.05	220	19	42	281	3.6	28.1	09.3
	1.40	332	17	33	382	6.6	38.2	10.4
	1.75	444	16	38	498	8.2	49.8	09.9
	2.10	511	14	51	576	7.8	57.6	09.6
	2.45	558	12	52	622	8.7	62.2	08.8
	2.80	585	32	39	656	8.2	65.6	08.2
	3.15	611	46	27	684	8.3	68.4	07.6
	3.50	655	55	19	729	8.8	72.9	07.3

[a] Reaction conditions: Catalyst (0.35×10^{-3} mmol dm^{-3}), Substrate (0.35 mol dm^{-3} to 3.5 mol dm^{-3}), Oxidant (0.35 mol dm^{-3}) in DCM : ACN solvent mixture (3 : 1 v/v); [b] -ol = cyclohexanol and -one = cyclohexanone; [c] Total TON = no. of mmol of product/no. of mmol of catalyst; [d] A/K = TON of -ol/(TON of -one + TON of ε-caprolactone); [e] Yield based on the oxidant; [f] Yield based on the substrate.

Table 7 Products of oxidation of cyclohexane catalyzed[a] by Ni(II) complexes

Complex	Cyclohexane (TON)			Total TON[c]	Chloro-benzene	A/K[d]	Yield[e] (%)
	-ol[b]	-one[b]	ε-caprolactone				
Blank	1.5	0.5	—	2			
1	558	12	52	622	395	8.7	62.2
1a	479	42	62	583	409	4.6	58.3
2	480	11	46	537	324	8.4	53.7
3	485	15	78	578	346	5.2	57.8
4	365	13	50	428	256	5.7	42.8
5	406	20	50	476	265	5.8	47.6
6	280	34	25	339	288	4.7	33.9
7	450	20	35	505	336	8.1	50.5

[a] Reaction conditions: Catalyst (0.35×10^{-3} mmol dm^{-3}), Substrate (2.45 mol dm^{-3}), Oxidant (0.35 mol dm^{-3}) in DCM : ACN solvent mixture (3 : 1 v/v); [b] -ol = cyclohexanol and -one = cyclohexanone; [c] Total TON = no. of mmol of product/no. of mmol of catalyst; [d] A/K = TON of -ol/(TON of -one + TON of ε-caprolactone); [e] Yield based on the oxidant.

Catalytic oxidation of alkanes

The experimental conditions and the results of catalytic oxidation of alkanes into alcohols for all the nickel(II) complexes are summarized in Tables 5–9. The conversion of alkanes into hydroxylated products was quantified based on gas chromatographic analysis by using authentic samples and an internal standard. The catalytic ability of the Ni(II) complexes towards oxidation of alkanes such as cyclohexane, adamantane, ethylbenzene and cumene was explored by using *m*-CPBA, H_2O_2 and *t*-BuOOH as oxidants in a dichloromethane/acetonitrile solvent mixture (3 : 1 v/v) at room temperature under nitrogen atmosphere. It has been reported[82] that *m*-CPBA is a very strong oxidizing agent towards oxidation of cyclohexane and adamantane to the corresponding alcohols and ketones in the absence of any metal catalyst, but only under vigorous reaction conditions including very high concentrations of *m*-CPBA, long reaction times and high temperatures. However, in control reactions performed in the absence of the Ni(II) complexes with *m*-CPBA as oxidant we observed only very small amounts of the oxidized products for all the substrates (Cyclohexane, 2 TON; Adamantane, 5 TON; Ethylbenzene, 10 TON; Cumene, 1 TON). This reveals that all the Ni(II) complexes act as catalysts towards the oxidation of alkanes to alcohols. In the presence of the complexes the oxidation of cyclohexane proceeds to give

Table 8 Products of oxidation of adamantane catalyzed[a] by Ni(II) complexes

Complex	Adamantane (TON)			Total TON[c]	Selectivity[d]	Yield[e] (%)
	1-adol[b]	2-adol[b]	2-adone[b]		3°/2°	
Blank	3.2	1.4	0.4	5		
1	516	113	10	639	12.5	63.9
1a	390	68	18	468	13.6	47.6
2	546	99	11	656	14.8	65.6
3	504	94	8	606	14.8	60.6
4	426	67	11	504	16.3	50.4
5	498	73	13	584	17.3	58.4
6	330	58	10	398	14.5	39.8

[a] Reaction conditions: Catalyst (0.2×10^{-3} mmol dm^{-3}), Substrate (0.4 mol dm^{-3}), Oxidant (0.2 mol dm^{-3}) in DCM : ACN solvent mixture (3 : 1 v/v); [b] 1-adol = 1-adamantanol, 2-adol = 2-adamantanol and 2-adone = 2-adamantanone; [c] TON = no. of mmol of product/no. of mmol of catalyst; [d] 3°/2° = (TON of 1-adol × 3)/(TON of 2-adol + TON of 2-adone); [e] Yield based on the oxidant.

Table 9 Oxidation products of ethylbenzene and cumene catalysed[a] by Ni(II) complexes

Complex	Ethylbenzene (TON)					Cumene		
	1-Phenyl- ethanol	Aceto- phenone	Total TON[b]	A/K[c]	Yield[d] (%)	2-Phenyl-2-propanol	Total TON[b]	Yield[d] (%)
Blank	5.1	4.9	10			1	1	
1	347	96	443	3.6	44.3	438	438	43.8
1a	290	88	378	3.3	37.8	316	316	31.6
2	303	132	435	2.3	43.5	361	361	36.1
3	280	135	415	2.0	41.5	348	348	34.8
4	204	129	333	1.6	33.3	280	280	28.0
5	212	110	322	1.9	32.2	298	298	29.8
6	178	106	284	1.6	28.4	268	268	26.8

[a] Reaction conditions: Catalyst (0.35×10^{-3} mmol dm^{-3}), Substrate (2.45 mol dm^{-3}), Oxidant (0.35 mol dm^{-3}) in DCM : ACN solvent mixture (3 : 1 v/v); [b] Total TON = no. of mmol of product/no. of mmol of catalyst; [c] A/K = TON of 1-phenylethanol/TON of acetophenone; [d] Yield based on the oxidant.

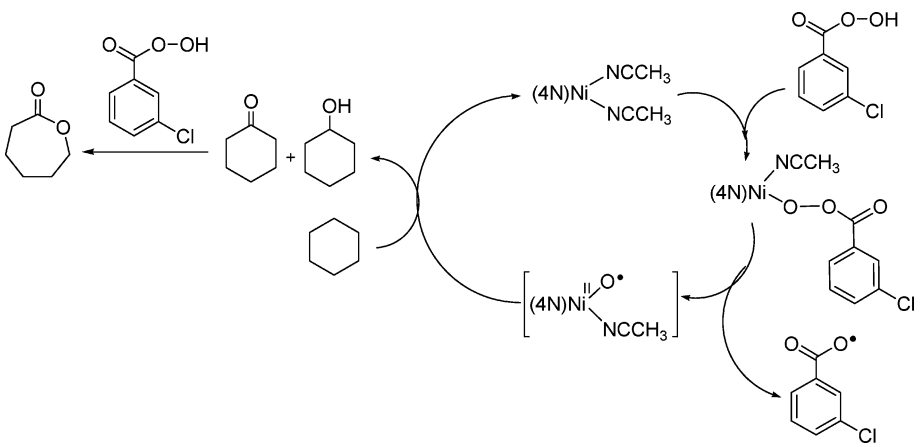

Scheme 2 Proposed mechanism of alkane hydroxylation.

cyclohexanol as the major product along with cyclohexanone and ε-caprolactone as the minor products, where ε-caprolactone is the over oxidized product of the oxidation of cyclohexanone by excess or unreacted *m*-CPBA. It is well known that *m*-CPBA is a quantitative reagent for the conversion of cyclic ketones to the corresponding lactones (Bayer–Villiger oxidation) in the absence of any metal catalyst and so the ε-caprolactone is not the metal catalyzed product. Interestingly, only 50% of the oxidized products are formed under air. Also, when H_2O_2/*t*-BuOOH is used as the oxidant only trace amounts of the oxidized products are formed, revealing that the Ni(II) complexes are not effective as catalysts for these oxidants.

The complex **1** catalyses the oxidation of cyclohexane to 558 TON of cyclohexanol (A) and 12 TON of cyclohexanone (K) and 52 TON of ε-caprolactone (A/K, 8.7). As proposed earlier,[68] we suggest that *m*-CPBA binds with Ni(II) in the catalyst by replacing a labile acetonitrile molecule to form the adduct $[Ni^{II}(L)(CH_3CN)(OOCOC_6H_4Cl)]^+$, which undergoes O–O bond homolysis leading to the formation of the reactive intermediate species and *m*-chlorobenzoic acid radical (Scheme 2). The species

$[(4N)(CH_3CN)Ni\text{-}O^{\bullet}]^+$ would then be involved in selective hydroxylation of alkanes, while *m*-chlorobenzoic acid radical undergoes decarboxylation to form chlorobenzene in greater than 60% yield. The observation of chlorobenzene supports the involvement of the intermediate species $[(4N)(CH_3CN)Ni\text{-}O^{\bullet}]^+$ in catalysis and indicates that *m*-chlorobenzoate radical is not the reactive intermediate, because it readily undergoes decarboxylation rather than hydrogen abstraction from the alkane.

The time course of the TON for **1** in cyclohexane oxidation is shown in Fig. 6, which clearly indicates that the catalytic activity of the Ni(II) complexes gradually proceeds even after 60 min. Also, upon increasing the substrate loading from 2.45 mol dm^{-3} to 3.50 mol dm^{-3} (Table 6), the catalytic activity increases from the total TON of 622 to 730 but with the same alcohol selectivity (A/K, 8.8). The very good A/K value observed indicates the absence of any free radical auto-oxidation. Interestingly, upon replacing the tetraphenylborate counter anion in **1** by perchlorate, as in **1a**, the total TON decreases appreciably to 479, with the selectivity also decreasing enormously to 4.6 and the yield of ε-caprolactone increasing to 62 TON. This shows that the perchlorate counter anion is coordinated in solution and retards the ligand exchange process with the oxidant *m*-CPBA (Scheme 2). However, when the number of equivalents of *m*-CPBA is increased, with an aim to increase the concentration of the intermediate and hence the reactivity, the amount of ε-caprolactone formed increases as a result of secondary oxidation of cyclohexanone by the increased oxidant concentration.

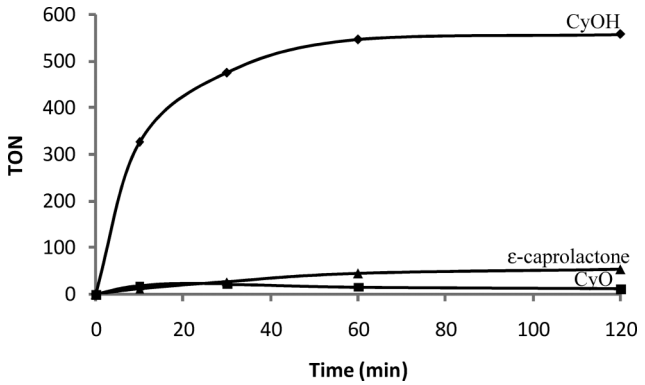

Fig. 6 Time dependent oxidation of cyclohexane catalyzed by **1** with *m*-CPBA.

Effect of supporting ligands

It is interesting to compare the catalytic behavior of **1** towards hydroxylation of cyclohexane with those of related nickel(II) catalysts **2–7** under identical conditions. Upon replacing the $-NMe_2$ group in **1** by an $-NEt_2$ group to give **2**, the product yields observed for cyclohexane oxidation are 480 TON of cyclohexanol, 11 TON of cyclohexanone and 46 TON of ε-caprolactone (Total TON, 537; A/K, 8.4). This illustrates that the increase in steric bulk of the nitrogen donor around Ni(II) renders its coordination to Ni(II) weaker (*cf.* above), enhancing the Lewis acidity of Ni(II) center further and decreasing the stability of the $[(4N)(CH_3CN)Ni\text{–}O^{\bullet}]^+$ species and hence the catalytic activity. Also, the steric bulk of the $-NEt_2$ group may contribute to the decreased binding of *m*-CPBA to Ni(II). Upon replacing one of the pyridylmethyl arms in **1** by an imidazolylmethyl arm to give **3**, cyclohexane is catalytically oxidized to cyclohexanol (485 TON) and cyclohexanone (15 TON) and ε-caprolactone (78 TON), revealing that the catalytic activity (Total TON, 578) decreases with a very significant decrease in alcohol selectivity (A/K, 5.2). Upon lowering the Lewis acidity of the Ni(II) center by the strongly σ-bonding imidazole donor (*cf.* above), the catalytic activity is expected to increase by enhancing the ligand exchange process, but a decrease in catalytic activity is observed. Also, upon replacing both the pyridylmethyl arms in **1** by imidazolylmethyl arms to give **4**, cyclohexane is converted to 365 TON of cyclohexanol and 13 TON of cyclohexanone and 50 TON of ε-caprolactone (Total TON, 428; A/K, 5.7). In this case also, upon decreasing the Lewis acidity of the Ni(II) center, the catalytic activity is lowered with only a small increase in selectivity. It is expected that the decrease in Lewis acidity of the Ni(II) center and the absence of π-back bonding pyridine donors may destabilize the reactive intermediate species $[(4N)(CH_3CN)Ni\text{–}O^{\bullet}]^+$ leading to a decrease in the reactivity. Upon replacing both the pyridylmethyl arms in **1** by quinolylmethyl arms to give **5**, cyclohexane is oxidized to 406 TON of cyclohexanol and 20 TON of cyclohexanone and 50 TON of ε-caprolactone (A/K, 5.8) with a decrease in catalytic activity (Total TON, 476). Obviously, the steric hindrance of the bulky quinolylmethyl arms to the binding of *m*-CPBA becomes significant. So, it is expected that the Ni(II) complex of a supporting ligand with strongly σ-bonding phenolate donor(s) would act as a poor catalyst. However, it has been reported[69] that the Ni(II)-bis(phenolate) complexes act as better catalysts than $[Ni(TPA)(OAc)(H_2O)]BPh_4$. It is possible that the phenolate donors remain protonated in solution also.

Under conditions identical to those used for **1**, the complex $[Ni(L7)(CH_3CN)_2](BPh_4)_2$ **7** catalyses the oxidation of cyclohexane to cyclohexanol with a total TON of only 505 with almost the same selectivity (A/K, 8.1) illustrating that the third pyridyl nitrogen donor located *cis* to the other two pyridyl nitrogen donors at a longer distance[67] is not effective in π-back bonding and hence a decrease in stability of the reactive intermediate species $[(4N)(CH_3CN)Ni\text{–}O^{\bullet}]^+$ leading to a decrease in reactivity of **7**. Also, upon replacing the weakly[83] coordinating $-NMe_2$ group in **1** by the pyridyl moiety as in $[Ni(L7)(CH_3CN)_2]^{2+}$ **7**, the Ni(II) center is rendered slightly less Lewis acidic, which does not facilitate substitution of coordinated CH_3CN by the oxidant *m*-CPBA. A similar lower catalytic activity is observed for **6** with three benzimidazolyl nitrogen donors. Upon replacing all the three pyridylmethyl arms in $[Ni(L7)(CH_3CN)_2]^{2+}$ **7** by benzimidazolylmethyl arms to give **6**, cyclohexane is oxidized to only 280 TON of cyclohexanol, 34 TON of cyclohexanone and 25 TON of ε-caprolactone, revealing a large decrease in both the catalytic activity (Total TON, 339) and selectivity (A/K, 4.7). It is clear that steric hindrance to *m*-CPBA binding by the bulky benzimidazolyl moiety and the decrease in both the Lewis acidity of the Ni(II) center and metal–ligand covalency become significant in determining the catalysis. However, the complex $[Ni(TPA)(OAc)(H_2O)]BPh_4$ oxidizes[67] cyclohexane to cyclohexanol with a higher total TON of 656, but the alcohol selectivity remains almost the same (A/K, 8.5). It is possible that the coordinated acetate ion, unlike ClO_4^- in **1a**, may a play a role in facilitating the binding of *m*-CPBA.

All the above observations reveal that the replacement of a pyridyl donor bound to Ni(II) by a weakly coordinating

–NMe_2/–NEt_2 group enhances the Lewis acidity of the Ni(II) center and encourages the binding of *m*-CPBA, whereas replacement by a strongly σ-bonding (benz)imidazolyl moiety enhances the electron density on the Ni(II) center leading to the weaker binding of *m*-CPBA. Also, a higher Lewis acidity of the Ni(II) center stabilizes the $[(4N)(CH_3CN)Ni\text{-}O^{\bullet}]^+$ species leading to a higher catalytic activity towards cyclohexane oxidation with *m*-CPBA as oxidant. Furthermore, a π-accepting ligand donor such as pyridine stabilizes the reactive radical intermediate $[(4N)(CH_3CN)Ni–O^{\bullet}]^+$ leading to a higher TON in the catalytic oxidation of hydrocarbons, while a σ-donor ligand destabilizes it leading to a decreased TON. Moreover, a bulky quinolyl/benzimidazolyl moiety sterically hinders binding of *m*-CPBA to Ni(II) center leading to a decrease in the catalytic activity. Very interestingly, a linear correlation between the metal–ligand covalency parameter β and TON is obtained (Fig. 7); however, complex **4** shows, in spite of a higher metal–ligand covalency parameter β due to two imidazolyl nitrogen donors, a lower TON, and this may be because of the lower Lewis acidity of the Ni(II) center due to the strongly σ-bonding imidazolyl nitrogen donors (*cf.* above). Thus, it is evident that a π-accepting ligand donor such as pyridine and/or a weakly coordinating–NMe_2/–NEt_2 donor is needed to achieve a higher catalytic activity by stabilizing the reactive intermediate $[(4N)(CH_3CN)Ni^{II}–O^{\bullet}]^+$ involved in the catalytic oxidation of hydrocarbons.

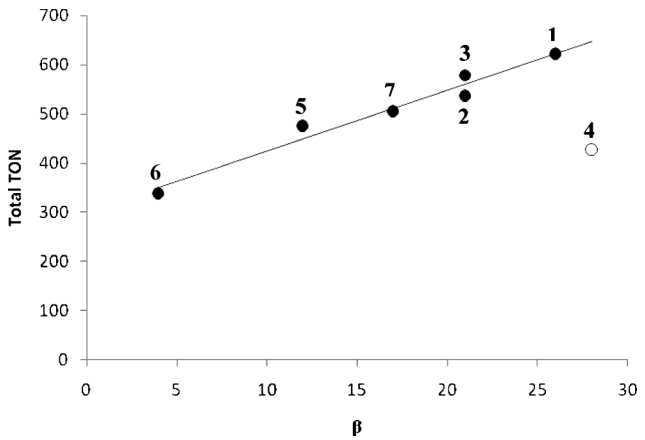

Fig. 7 Correlation of TON with metal–ligand covalency parameter β.

Adamantane oxidation

The catalytic activity of all the Ni(II) complexes towards oxidation of adamantane has been also explored and the results are summarized in Table 8. All the Ni(II) complexes catalyse the oxidation of adamantane efficiently to give 1-adamantanol and 2-adamantanol as the major products along with 2-adamantanone as the minor product. Complex **1** catalyzes the oxidation of adamantane to give 516 TON of 1-adamantanol, 113 TON of 2-adamantanol and 10 TON of 2-adamantanone with a good selectivity (3°/2°, 12.5). However, **1a** catalyzes adamantane oxidation to give 390 TON of 1-adamantanol, 68 TON of 2-adamantanol and 10 TON of 2-adamantanone with a significant decrease in catalytic activity (Total TON, 468). As in the case of cyclohexane oxidation, the complex with tetraphenyl borate counter anion acts as a more efficient catalyst than the perchlorate complex **1a** in adamantane oxidation also but with almost the same selectivity. However, **2** catalyses adamantane oxidation to 650 TON, which is higher than that for **1**. All the other complexes also catalyze the oxidation with good TON and high 3°/2° ratio. Thus, upon exchanging a donor around Ni(II) for a stronger donor, the 3°/2° ratio increases gradually from 12.5 up to 17.0. The high 3°/2° selectivity observed indicates involvement of the $[(4N)(CH_3CN)Ni–O^{\bullet}]^+$ species as metal-based oxidant in adamantane oxidation also.

The catalytic activities of the Ni(II) complexes were further explored for the oxidation of ethylbenzene and cumene and the results are summarized in Table 9. All the Ni(II) complexes catalyse the oxidation of ethylbenzene to give 2-phenylethanol and acetophenone but with moderate selectivity only. Additionally, they catalyze the oxidation of cumene selectively to form 2-phenyl-2-propanol without any side product formation.

Conclusions

Several nickel(II) complexes derived from tripodal tetradentate 4N ligands have been isolated and their ability to carry out alkane functionalization was studied using *m*-CPBA as an oxidant. All the Ni(II) complexes with distorted octahedral coordination geometry catalyze the hydroxylation of the alkanes cyclohexane, adamantane, ethylbenzene and cumene using *m*-CPBA as oxidant. The observed variation in alcohol selectivity for cyclohexane oxidation suggests the involvement of a metal-based oxidant rather than a freely diffusing radical in the reaction. The ligand stereoelectronic factors and Lewis acidity of the Ni(II) center are found to be significant in determining the catalytic activity as well as the selectivity of alkane oxidation. For adamantane oxidation, however, the incorporation of a sterically hindering quinolyl/benzimidazolyl moiety to support Ni(II) leads to a high 3°/2° bond selectivity. A linear correlation between the metal–ligand covalency parameter (β) and the turnover number has been observed.

Acknowledgements

We sincerely thank the Department of Science and Technology, New Delhi, for a Pre-doctoral Fellowship [Scheme No. SR/S1/PRD-04/2006] to M.B under new Initiatives in Bioinorganic Chemistry and for supporting this research [Scheme No. SR/S5/BC-05/2006]. This work was also supported by Indo-French Centre (IFCPAR) [Scheme No. IFC/A/4109-1/2009/993]. Professor M. Palaniandavar is a recipient of a DST Ramanna Fellowship [Scheme No. SR/S1/RFIC-01/2007 and SR/S1/RFIC-01/2010]. We thank Department of Science and Technology (FIST program), New Delhi for the use of the diffractometer in our School of Chemistry.

References

1 J. Colby, H. Dalton and R. Whittenbury, *Annu. Rev. Microbiol.*, 1979, **33**, 481.
2 H. Dalton, *Adv. Appl. Microbiol.*, 1980, **26**, 71.
3 J. B. Vincent, G. L. Olivier-Lilley and B. A. Averill, *Chem. Rev.*, 1990, **90**, 1447.
4 J. D. Lipscomb, *Annu. Rev. Microbiol.*, 1994, **48**, 317.
5 A. L. Feig and S. J. Lippard, *Chem. Rev.*, 1994, **94**, 759.
6 B. J. Waller and J. D. Lipscomb, *Chem. Rev.*, 1996, **96**, 2625.

7 M. Baik, M. Newcomb, R. A. Friesner and S. J. Lippard, *Chem. Rev.*, 2003, **103**, 2385.
8 M. Costas, M. P. Mehn, M. P. Jensen and L. Que Jr, *Chem. Rev.*, 2004, **104**, 939.
9 E. Y. Tshuva and S. J. Lippard, *Chem. Rev.*, 2004, **104**, 987.
10 S. V. Kryatov, E. V. Rybak-Akimova and S. Schindler, *Chem. Rev.*, 2005, **105**, 2175.
11 J. H. Green and H. Dalton, *J. Biol. Chem.*, 1989, **264**, 17698.
12 N. Kitajima, H. Fukui and Y. Moro-oka, *J. Chem. Soc., Chem. Commun.*, 1988, 485.
13 W. Nam, R. Ho and J. S. Valentine, *J. Am. Chem. Soc.*, 1991, **113**, 7052.
14 N. Kitajima, M. Ito, H. Fukui and Y. Moro-oka, *J. Chem. Soc., Chem. Commun.*, 1991, 102.
15 M. Kodera, H. Shimakoshi and K. Kano, *Chem. Commun.*, 1996, 1737.
16 K. Chen and L. Que Jr., *Chem. Commun.*, 1999, 1375.
17 K. Chen and L. Que Jr., *Angew. Chem., Int. Ed.*, 1999, **38**, 2227.
18 Y. Jin and J. D. Lipscomb, *J. Biol. Inorg. Chem.*, 2001, **6**, 717.
19 K. Chen and L. Que Jr, *J. Am. Chem. Soc.*, 2001, **123**, 6327.
20 Y. Mekmouche, S. Ménage, C. Toia-Duboc, M. Fontecave, J.-B. Galey, C. Lebrun and J. Pécaut, *Angew. Chem., Int. Ed.*, 2001, **40**, 949.
21 W. Nam, J. Y. Ryu, I. Kim and C. Kim, *Tetrahedron Lett.*, 2002, **43**, 5487–5490.
22 K. Chen, M. Costas and L. Que Jr, *J. Chem. Soc., Dalton Trans.*, 2002, 672.
23 W. J. Song, Y. O. Ryu, R. Song and W. Nam, *J. Biol. Inorg. Chem.*, 2005, **10**, 294.
24 G. Xue, R. D. Hont, E. Münck and L. Que Jr, *Nat. Chem.*, 2010, **2**, 400.
25 D. Riley, M. Stern and J. Ebner, in *The Activation of Dioxygen and Homogeneous Catalytic Oxidation*, ed. D. H. R. Barton, A. E. Martell and D. T. Sawyer, Plenum, New York, 1993, p. 31.
26 M. Costas, K. K. Chen and L. Que Jr., *Coord. Chem. Rev.*, 2000, **200**, 517.
27 D. H. R. Barton and D. Doller, *Acc. Chem. Res.*, 1992, **25**, 504.
28 A. E. Shilov and A. A. Shteinman, *Acc. Chem. Res.*, 1999, **32**, 763.
29 P. Stavropoulos, R. Çelenligil-Çetin and A. E. Tapper, *Acc. Chem. Res.*, 2001, **34**, 745.
30 T. Punniyamurthy, S. Velusamy and J. Iqbal, *Chem. Rev.*, 2005, **105**, 2329.
31 H. Komatsuzaki, N. Sakamoto, M. Satoh, S. Hikichi, M. Akita and Y. Moro-oka, *Inorg. Chem.*, 1998, **37**, 6554.
32 M. S. Seo, J. Y. Kim, J. Annaraj, Y. Kim, Y. Lee, S. Kim, J. Kim and W. Nam, *Angew. Chem., Int. Ed.*, 2007, **46**, 377.
33 K. Nehru, S. J. Kim, I. Y. Kim, M. S. Seo, Y. Kim, S. Kim, J. Kim and W. Nam, *Chem. Commun.*, 2007, 4623.
34 F. A. Chavez and P. K. Mascharak, *Acc. Chem. Res.*, 2000, **33**, 539.
35 W. Nam, I. Kim, Y. Kim and C. Kim, *Chem. Commun.*, 2001, 1262.
36 N. Kitajima, K. Fujisawa and Y. Moro-oka, *J. Am. Chem. Soc.*, 1989, **111**, 8975.
37 R. R. Jacobson, Z. Tyeklar, A. Farooq, K. D. Karlin, S. Liu and J. Zubieta, *J. Am. Chem. Soc.*, 1988, **110**, 3690.
38 N. W. Aboelella, S. V. Kryatov, B. F. Gherman, W. W. Brennessel, V. G. Young Jr., R. Sarangi, E. V. Rybak-Akimova, K. O. Hodgson, B. Hedman, E. I. Solomon, C. J. Cramer and W. B. Tolman, *J. Am. Chem. Soc.*, 2004, **126**, 16896.
39 L. M. Mirica, X. Ottenwaelder and T. D. P. Stack, *Chem. Rev.*, 2004, **104**, 1013.
40 L. Que Jr. and W. B. Tolman, *Angew. Chem., Int. Ed.*, 2002, **41**, 1114.
41 M. Suzuki, *Acc. Chem. Res.*, 2007, **40**, 609.
42 C. J. Cramer and W. B. Tolman, *Acc. Chem. Res.*, 2007, **40**, 601.
43 S. Itoh and S. Fukusumi, *Acc. Chem. Res.*, 2007, **40**, 592.
44 T. Kojima, *Chem. Lett.*, 1996, 121.
45 T. Kojima, H. Matsuo and Y. Matsuda, *Inorg. Chim. Acta*, 2000, **300–302**, 661.
46 J. R. Bryant, T. Matsuo and J. M. Mayer, *Inorg. Chem.*, 2004, **43**, 1587.
47 M. Yamaguchi, H. Kousaka, S. Izawa, Y. Ichii, T. Kumano, D. Masui and T. Yamagishi, *Inorg. Chem.*, 2006, **45**, 8342.
48 T. Kojima, K. Hayashi, S. Iizuka, F. Tani, Y. Naruta, M. Kawano, Y. Ohashi, Y. Hirai, K. Ohkubo, Y. Matsuda and S. Fukuzumi, *Chem.–Eur. J.*, 2007, **13**, 8212.
49 T. Okumura, Y. Morishima, H. Shiozaki, T. Yagyu, Y. Funahashi, T. Ozawa, K. Jitsukawa and H. Masuda, *Bull. Chem. Soc. Jpn.*, 2007, **80**, 507.
50 S. Yiu, W. Man and T. Lau, *J. Am. Chem. Soc.*, 2008, **130**(32), 10821.
51 D. Schröder and H. Schwarz, *Angew. Chem., Int. Ed. Engl.*, 1995, **34**, 1973.
52 K. Jitsukawa, Y. Oka, S. Yamaguchi and H. Masuda, *Inorg. Chem.*, 2004, **43**, 8119.
53 M. Murali, R. Mayilmurugan and M. Palaniandavar, *Eur. J. Inorg. Chem.*, 2009, **22**, 3238.
54 J. F. Kinneary, J. S. Albert and C. J. Burrows, *J. Am. Chem. Soc.*, 1988, **110**, 6124.
55 S. Hikichi, M. Yoshizawa, Y. Sasakura, M. Akita and Y. Moro-oka, *J. Am. Chem. Soc.*, 1998, **120**, 10567.
56 K. Shiren, S. Ogo, S. Fujinami, H. Hayashi, M. Suzuki, A. Uehara, Y. Watanabe and Y. Moro-oka, *J. Am. Chem. Soc.*, 2000, **122**, 254.
57 B. S. Mandimutsira, J. L. Yamarik, T. C. Brunold, W. Gu, S. P. Cramer and C. G. Riordan, *J. Am. Chem. Soc.*, 2001, **123**, 9194.
58 S. Hikichi, M. Yoshizawa, Y. Sasakura, H. Komatsuzaki, Y. Moro-oka and M. Akita, *Chem.–Eur. J.*, 2001, **7**, 5011.
59 K. Fujita, R. Schenker, W. Gu, T. C. Brunold, S. P. Cramer and C. G. Riordan, *Inorg. Chem.*, 2004, **43**, 3324.
60 J. Cho, H. Furutachi, S. Fujinami and M. Suzuki, *Angew. Chem., Int. Ed.*, 2004, **43**, 3300; J. Cho, H. Furutachi, S. Fujinami and M. Suzuki, *Angew. Chem.*, 2004, **116**, 3362.
61 M. T. Kieber-Emmons, J. Annaraj, M. S. Seo, K. M. Van Heuvelen, T. Tosha, T. Kitagawa, T. C. Brunold, W. Nam and C. G. Riordan, *J. Am. Chem. Soc.*, 2006, **128**, 14230.
62 M. T. Kieber-Emmons and C. G. Riordan, *Acc. Chem. Res.*, 2007, **40**, 618.
63 S. Yao, E. Bill, C. Milsmann, K. Wieghardt and M. Driess, *Angew. Chem., Int. Ed.*, 2008, **47**, 7110; S. Yao, E. Bill, C. Milsmann, K. Wieghardt and M. Driess, *Angew. Chem.*, 2008, **120**, 7218.
64 A. Company, S. Yao, K. Ray and M. Driess, *Chem.–Eur. J.*, 2010, **16**, 9669.
65 S. Hikichi, C. Kobayashi, M. Yoshizawa and M. Akita, *Chem.–Asian J.*, 2010, **5**, 2086.
66 T. Tano, Y. Doi, M. Inosako, A. Kunishita, M. Kubo, H. Ishimaru, T. Ogura, H. Sugimoto and S. Itoh, *Bull. Chem. Soc. Jpn.*, 2010, **83**, 530.
67 T. Nagataki, Y. Tachi and S. Itoh, *Chem. Commun.*, 2006, 4016.
68 T. Nagataki, K. Ishii, Y. Tachi and S. Itoh, *Dalton Trans.*, 2007, 1120.
69 T. Nagataki and S. Itoh, *Chem. Lett.*, 2007, **36**(6), 748.
70 S. Hikichi, H. Okuda, Y. Ohzu and M. Akita, *Angew. Chem., Int. Ed.*, 2009, **48**, 188.
71 G. J. P. Britovsek, J. England and A. J. P. White, *Inorg. Chem.*, 2005, **44**, 8125.
72 A. Raja, V. Rajendiran, P. Uma Maheswari, R. Balamurugan, C. A. Kilner, M. A. Halkrow and M. Palaniandavar, *J. Inorg. Biochem.*, 2005, **99**, 1717.
73 L. K. Thompson, B. S. Ramaswamy and E. A. Seymour, *Can. J. Chem.*, 1977, **55**, 878.
74 G. M. Sheldrick, *SAINT 5.1 ed.*, Siemens Industrial Automation Inc., Madison, WI, 1995.
75 *SADABS, empirical absorption Correction Program*, University of Göttingen, Göttingen, Germany, 1997.
76 G. M. Sheldrick, *SHELXTL Reference Manual: Version 5.1*, Bruker AXS, Madison, WI, 1997.
77 G. M. Sheldrick, *SHELXL-97: Program for Crystal Structure Refinement*, University of Göttingen, Göttingen, Germany, 1997.
78 M. Velusamy, M. Palaniandavar and K. R. Justin Thomas, *Polyhedron*, 1998, **17**, 2179.
79 A. B. P. Lever, *Inorganic Electronic Spectroscopy*, Elsevier (Second Edition), Amsterdam, 1986.
80 A. B. P. Lever, *J. Chem. Educ.*, 1968, **45**, 711.
81 D. R. Brown and R. R. Pavlis, *J. Chem. Educ.*, 1985, **62**, 807.
82 A. Bravo, H.-R. Bjorsvik, F. Fontana, F. Minisci and A. Serri, *J. Org. Chem.*, 1996, **61**, 9409.
83 M. Velusamy and M. Palaniandavar, *Inorg. Chem.*, 2003, **42**, 8283.

